Oblique rifting of the Equatorial Atlantic: Why there is no Saharan Atlantic Ocean

Christian Heine[1], Sascha Brune[2,1]

[1] *EarthByte Group, School of Geosciences, The University of Sydney, NSW 2006, Australia*

[2] *Helmholtz Centre Potsdam, GFZ German Research Centre for Geosciences, Section 2.5, Geodynamic Modelling, Potsdam, Germany*

ABSTRACT

Rifting between large continental plates results in either continental breakup and the formation of conjugate passive margins or rift abandonment and a set of aborted rift basins. The driving mechanisms behind "successful" or "failed" rifting have so far never been scrutinized by joint kinematic and forward numerical modelling. We analyse the Early Cretaceous extension between Africa and South America which was preceded by about 20-30 Myrs of extensive rifting prior to the final separation between the two plates. While the South and Atlantic conjugate margins continued into seafloor spreading mode, forming the Atlantic ocean basin, Cretaceous-aged African intraplate rifts eventually "failed" soon after South America broke up from Africa. We address the spatio-temporal dynamics of rifting in domains by comparing a new plate kinematic model for the South Atlantic and 3D forward rift models. This joint approach elucidates (1) the dynamic competition of Atlantic and extensional systems, (2) two stage kinematics of the South Atlantic rift system, and (3) the acceleration of the South American plate prior to final break-up. We suggest that obliquity the success of the Equatorial Atlantic rift, ultimately prohibiting the formation of a "Saharan Atlantic Ocean" in the Early Cretaceous, and exerting a primary control on the increase in observed extensional velocities between the South American and African plates. Our results imply that rift obliquity acts as selector between successful ocean basin formation and "failed rifts".

INTRODUCTION

Lithospheric extension related to the final dispersal of western Gondwana started with the formation of large intracontinental rift systems within and between the African and South American plates in the Early Cretaceous (Burke and Dewey, 1974; Unternehr et al., 1988; Fairhead, 1988). Four extensional domains with a number of individual basins developed due to relative motions between the main rigid continental lithospheric blocks during that time (Fig. 1a; Heine et al., 2013). These were: (1) the Central African Rift System (CARS), extending from Sudan to the eastern part of the Benoue Trough (Burke and Dewey, 1974; Fairhead, 1986; Genik, 1992; McHargue et al., 1992), (2) the West African Rift System (WARS), extending from the eastern part of the Benoue Trough northwards towards southern Libya (Fairhead, 1986; Genik, 1992), (3) the South Atlantic rift system (SARS) sensu strictu, comprising the present-day conjugate South Atlantic marginal basins with the Benoue Trough/NE Brazil at its northernmost extent (Nürnberg and Müller, 1991), and (4) the Equatorial Atlantic rift system (EqRS), covering the conjugate African and South American margins from the Guinea Plateau/Demarara Rise in the West to the Benoue Trough/NE'most Brazil in the East (Basile et al., 2005). While extension in the SARS and EqRS ultimately lead to the formation of the South and Equatorial Atlantic (Nürnberg and Müller, 1991; Torsvik et al., 2009; Moulin et al., 2009; Heine et al., 2013), the CARS and WARS never went beyond rift mode and eventually "failed", being preserved as subsurface graben structures (Burke and Dewey, 1974; Fairhead, 1986; Genik, 1992).

Here, we investigate the spatio-temporal evolution of continental extension which lead to the abandonment of these large intracontinental rift systems and the breakup of western Gondwana between Africa and South America along their present-day conjugate passive margins systems. We analyse the geodynamics of rifting prior and during breakup by combining plate kinematic and forward numerical models.

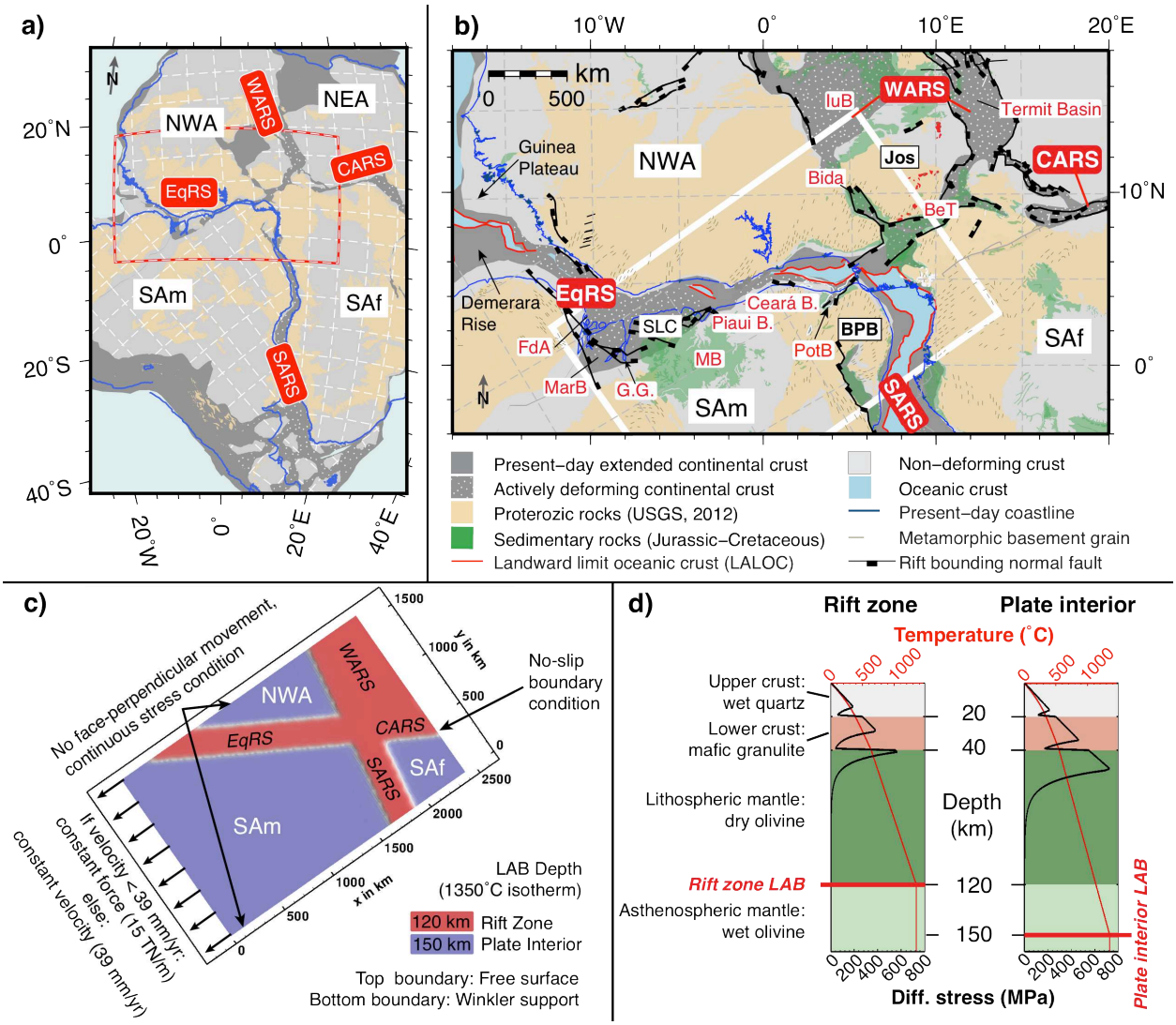

Figure 1: Overview map and numerical model setup. a) Lambert Azimuthal Equal Area view of pre-rift configuration at 140 Ma showing major rigid plates and deforming crustal regions (Heine et al., 2013). Present-day South America and African plates are separated into 4 major rigid plates in the region of interest during the Late Jurassic/Early Cretaceous: NEA – Northeast Africa, NWA - Northwest Africa, SAf - Southern Africa, SAm - South America. Rift systems (white font, red background): CARS – Central African rift, EqRS – Equatorial Atlantic rift, SARS – South Atlantic rift, WARS – West African rift. Southern Africa held fix in present-day position, red/white polygon indicates frame of map (b), white dashed lines are present-day 5˚ graticule; b) Reconstruction at 117 Ma with South Africa held fix in present-day coordinates (Heine et al., 2013). The northernmost segment of SARS is already in seafloor spreading mode, in the EqRS breakup is incipient. The numerically modeled key region is indicated by the thick white rectangle. Minor rigid plates: BPB - Borborema Province Block (NE Brazil), Jos - Jos Subplate in northern Nigeria, SLC - São Luis Craton. Present-day submarine features: DeR - Demarara Rise, GPl. - Guinea Plateau. Basins (red font, white background in annotation indicates active extension, grey background indicates tectonic quiescence at reconstruction time): BarB - Barreirinhas Basin, BeT - Benoue Trough, CdIGR - Côte d'Ivoire/Ghana Ridge, D/D B. - Doba/Doseo Basins, DGB - Deep Ghanaian Basin, FdA - Foz do Amazon, IuB - Iullemmeden Basin, KB - Keta/Togo/Benin Basin, MarB - Marajó Basin, PoT - Potiguar Basin, RTJ - Recôncavo/Tucano/Jaítoba Basins, Gao T. – Gao Trough; c) The initial geometric setup of the 3D numerical model involves prospective rift zones as thermal heterogeneities. Model size is 2400x1600 km horizontal and 200 km vertical; d) The lithospheric segment is vertically divided in four distinct petrological layers: upper crust, lower crust, lithospheric mantle, and asthenospheric mantle. Rheological parameters (see supplementary material) of the crust are chosen to represent a narrow rift setting as it is evident by the short amount of thinned continental crust along the conjugate Equatorial Margins (Azevedo, 1991). Rheology of lithospheric and asthenospheric mantle is based on laboratory creep measurements for dry and wet olivine, respectively.

PLATE KINEMATIC MODEL

Our study builds upon a new plate kinematic model for the evolution of the West Gondwana rift structures (SARS, CARS, WARS and EqRS), quantitatively integrating crustal deformation from Cretaceous African and South American intraplate deforming zones as well as from the conjugate passive margins of the Equatorial and South Atlantic (see supplementary material and Heine et al., 2013, for details). Stage poles of relative motions between the African plates, describing the lithospheric extension in the WARS and CARS, have been generated from published extension estimates (e.g. Genik, 1992; McHargue et al., 1992) and fitting of restored sediment basin widths (Heine et al., 2013). Angular velocities for the Cretaceous Magnetic Quiet Zone are linearly interpolated between magnetic anomalies M0 (120.6 Ma) and C34 (83.0 Ma).Relative motions between the main rigid plates are initiated at 140 Ma and progress at relatively slow extensional velocities, compounding to ≈4 mm a^{-1} between South America and Southern Africa until 126 Ma in a South Africa-fixed reference frame (full spreading rates computed at 37.5˚ W/5˚ S). Modeled plate motions between South America and NW Africa result in ≈10–15 km displacement during the initial phase. Crustal uplift, extension and volcanism observed in the Gurupi Graben, Marajo and Foz do Amazon Basins in Brazil during Berriasian to Hauterivian times, support early, likely rift- and transform-related deformation in the central Equatorial Atlantic region at low strain rates (Azevedo, 1994; Soares Júnior et al., 2011). Non-deforming South American and NW African plates surrounding this region (Heine et al., 2013) imply that an incipient, diffuse plate boundary along the future Equatorial Atlantic region must have existed during the Early Cretaceous, contemporaneous with rifting in the CARS and WARS. Isolated margin segments along the EqRS show evidence for increasing tectonism related to relative transtensional motions between South America and Africa from the Early Barremian onwards, (Basile et al., 2005) and peaking in Aptian times with major rift-related subsidence reported from all EqRS basins (Azevedo, 1991; Brownfield and Charpentier, 2006; Soares Júnior et al., 2011). Marine magnetic anomalies in the southernmost South Atlantic indicate northward propagating breakup followed by oceanic spreading in the southern South Atlantic rift segment (Nürnberg and Müller, 1991; Moulin et al., 2009; Heine et al., 2013), while the northern part of the South Atlantic segment still experiences continental extension (Torsvik et al., 2009; Moulin et al., 2009; Heine et al., 2013). Relative plate velocities based on the seafloor spreading patterns indicate a ≈10-fold increase of spreading/extensional velocities towards the beginning of the Cretaceous Normal Polarity Superchron (CNPS) at Base Aptian (120.6 Ma) from 4 mm a^{-1} to > 39 mm a^{-1} (Heine et al., 2013). Velocity increases of similar magnitude are modeled by other workers (Nürnberg and Müller, 1991; Torsvik et al., 2009) albeit using different absolute ages. The described evolution of relative extensional velocities is further supported by stratigraphic data along the conjugate South Atlantic margins indicating multiple subsidence phases in marginal basins (e.g. Karner and Driscoll, 1999).

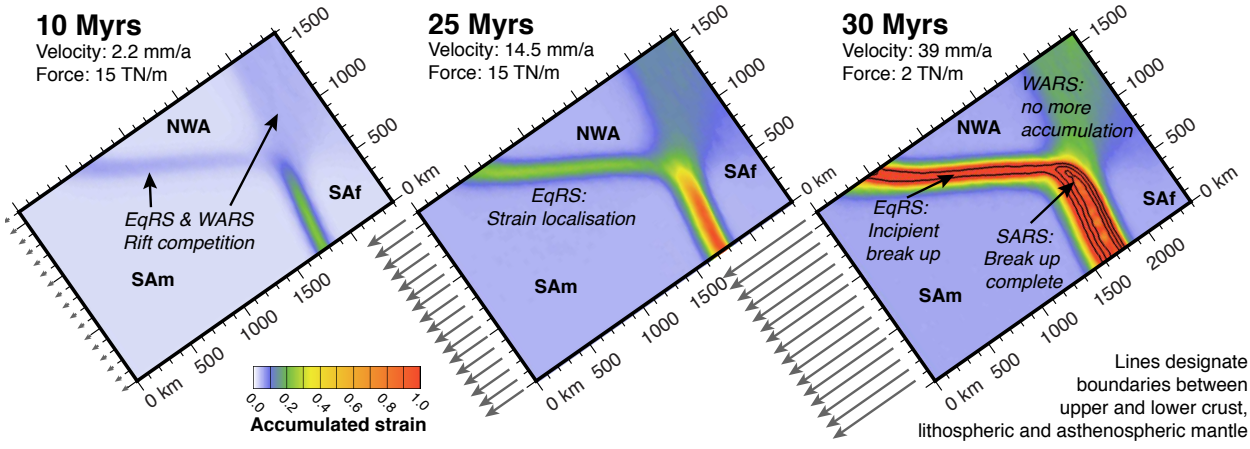

Figure 2: Accumulated strain over 30 Myrs after 10, 25 and 30 Myrs of model run time. Lines designate boundaries between upper crust, lower crust, lithospheric and asthenospheric mantle.

NUMERICAL MODEL SETUP

We investigate the dynamics of rift competition and the reason for the observed multi-phase velocity behaviour by means of a 3D thermo-mechanical model (Popov and Sobolev, 2008; for details see supplementary material). We adopt rift geometries of the Equatorial Atlantic region and thereby extend previous, fundamental simulations of oblique rifting (Brune et al., 2012; Brune and Autin, 2013). The model domain is oriented such that two edges are parallel to the extensional direction, comprising the rift zones of EqRS, WARS, CARS and SARS (Fig. 1a,b). Since Gondwana rifting re–activated predominantly Pan-African–aged mobile belts (Janssen et al., 1995), we introduce prospective rift zones by elevating the depth of the thermal lithosphere-asthenosphere boundary (1350° C) to 120 km in contrast to 150 km of the surrounding Proterozoic lithosphere (Fig. 1c; Artemieva, 2006). Each prospective rift in our study is represented by the same thermal heterogeneity (Fig. 1d). North of the Benoue Trough, Early Cretaceous intraplate magmatism of the Jos Plateau (Wilson and Guiraud, 1992) as well as faulting and subsidence in the Bida (Ojo, 1990; Genik, 1992) and Iullemmeden Basins (including the Gao Trough in Mali; Fig. 1b; Petters, 1981; Genik, 1992) confirm distributed extension west of the WARS and perturbance of lithospheric temperature gradients. We count this region to genetically belong to the WARS extensional domain and therefore simplify the complex junction of WARS and CARS (Fig. 1a,b) by homogeneously weak lithosphere (Fig. 1c). During the rift process, we keep the extensional force constant (15, 16 or 17 TN m^{-1}) allowing for self-consistent evolution of extensional velocities. Upon transition from rifting to seafloor spreading in nature, however, lithospheric strength at the plate boundary becomes negligible such that extensional velocities grow independent of the local stress balance. Instead they become affected primarily by global scale plate tectonic forcing (e.g. slab pull, mantle drag). We account for that transition by applying the force boundary condition only until velocities equate local seafloor spreading rates derived from the plate kinematic model (≈39 mm a^{-1}) and use this criteria to link numerical model time with the plate kinematic model to evaluate the spatio-temporal rift evolution (Fig. 3).

EVOLUTION OF THE EQUATORIAL ATLANTIC

We subsequently describe the evolution of our preferred numerical model (15 TN m^{-1}) and relate the results to plate kinematic model, and geological record (cf. supplementary material). Strain initially accumulates in our numerical model simultaneously along the three rift domains (SARS, EqRS, and the SW WARS; Fig. 2, 10 Myr model time). Modelled extensional velocities (2–4 mm a^{-1} full extension) for these domains are in accordance with slow rifting compared to the plate kinematic model (Fig. 3). After 25 Myrs of model time, strain increasingly starts to localise along the proto-Equatorial Atlantic (Fig. 2, cf. 122 Ma reconstruction), with the rift tip of the SARS taking a sharp turn to the West converging into the weakness zone of the Proto-Gulf of Guinea, while subtle extension continues to affect the WARS extensional domain. The numerical model suggests that the reason for increased strain accumulation in the EqRS and the simultaneous strain rate decrease in the WARS lies in their respective orientation towards plate divergence (EqRS: 60°, WARS: 30°) since all other parameters are the same. This is corroborated by analytical and numerical (Brune et al., 2012), as well as analogue (Chemenda et al., 2002) models, which show that highly oblique rifts are mechanically favoured. Both EqRS and WARS evolve in the numerical model according to their local extensional velocity that derives from the obliquity-dependent strength of the respective rift system. While rift velocities remain low and both rifts deform simultaneously until ≈25 Myr model time (Fig. 2), the highly oblique EqRS accumulates more strain causing lithospheric necking and strength loss. Subsequently, rifting accelerates in order to satisfy constant force boundary conditions. This non-linear feedback between lithospheric strength and extensional velocity results in a strong velocity increase between the African and South American plates (Fig. 3) once strain localises in the EqRS. From Barremian/Aptian times (≈123–112 Ma), rifting in most proximal parts of the Equatorial Atlantic marginal basins is observed, with block faulting, dextral shearing and reactivation of older lineaments progressively affecting the region from the Benoue Trough/NE Brazil in the East towards the conjugate Guinea Plateau/Demarara Rise (Mascle and Blarez,

1987; Azevedo, 1991; Basile et al., 2005; Soares Júnior et al., 2011). This phase is also consistent with increased subsidence reported from the northern South Atlantic conjugate margins (Karner and Driscoll, 1999) and full continental breakup and seafloor spreading in the northernmost SARS segment between the NE Brazil and Gabon/Cameroon margins (Heine et al., 2013). Full lithospheric breakup along the EqRS is achieved in our numerical model after 34 Myrs due to further strain localisation whereas post-rift thermal subsidence along the conjugate divergent Equatorial Atlantic marginal basins commences in late Aptian/early Albian times (Figs. 2, 30 Myr model, cf. 115 Ma reconstruction; Mascle and Blarez, 1987; Azevedo, 1991; Matos, 1992). In our plate reconstructions, oblique motion along the Côte d'Ivoire-Ghanaian Ridge causes transpression and uplift during the late Albian until full lithospheric separation between Africa and South America by around 104 Ma (see electronic supplements). This phase also coincides with a deceleration and subsequent counterclockwise rotation of the African plates in an absolute reference frame (Torsvik et al., 2008).

Note that the duration of the plate velocity increase in the numerical model compares excellent with independently derived kinematic plate reconstructions (Fig. 3; Nürnberg and Müller, 1991; Torsvik et al., 2009; Heine et al., 2013). Large parts of the Pacific South American margin, were experiencing extensional conditions prior to our modeled velocity increase. The acceleration of the South American plate from Aptian/Albian times onwards correlates well with a change to a predominantly compressional regime along the margin (Ramos, 2010; Maloney et al., 2013).

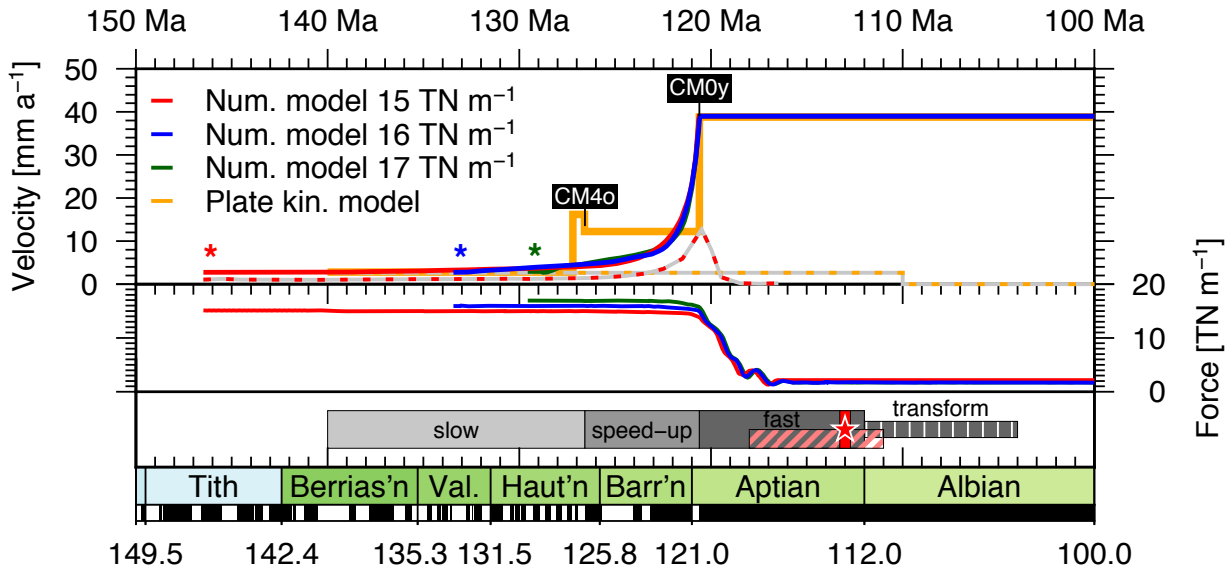

Figure 3: Velocities (top), forces (middle) and inferred continental deformation along the EqRS (bottom) for selected forward numerical models and plate kinematic model (only velocities). Full extensional velocity calculated from the plate kinematic models uses a point located on the present-day South American plate at 37.5˚W 5˚S and relative to a fixed Southern African plate. Magnetic anomalies: CM4o - Anomaly CM4 old end (126.57 Ma), CM0y - Anomaly CM0 young end (120.6 Ma). Stage pole for SAm-SAf rotations in plate model 1 is determined through cumulative extension in the WARS and CARS between the fit reconstruction (140 Ma) and CM4o position (126.57 Ma) and allows for transtensional motion between SAm and NWA. Stage rotations for CM4o and CM0y are derived from magnetic anomaly patterns in the southern South Atlantic (Moulin et al., 2009; Heine et al., 2013). Dashed velocity lines on gray background show relative motions between NW and NE Africa as proxy for extensional velocities in the WARS. Bottom: "Slow", "speed-up", and "fast" indicate relative extensional velocities between rift onset and breakup along EqRS. Red line and star denote predicted breakup from numerical model. Oblique stripe pattern indicates duration of diachronous breakup along the EqRS based on plate model. Chevron-pattern indicates transpressional phase along EqRS from plate model, "transform" and white vertical line pattern denote transform-stage after breakup occurred along passive margin segments. Timescale denotes geological stages, boxed white/black scale below denotes magnetic polarity chrons (black = normal polarity, white = reversed polarity) with absolute ages based on new hybrid timescale (Heine et al., 2013).

In order to constrain the effect of the boundary force, we re-compute the evolution of numerical models with different forces of 16 and 17 TN m^{-1} but otherwise identical parameters. We find that in both models the strength-velocity feedback initiates earlier break-up along the EqRS to 23 and 18 Myr model time, respectively (Fig. 3). However, the duration of the velocity increase remains the same indicating that it is solely affected by internal rift dynamics. At present, observations from the Equatorial Atlantic margins are ambivalent regarding the onset of rifting and support only minor tectonic activity at low strain rates before Late Barremian/Early Aptian times (Azevedo, 1991; Matos, 1992; Basile et al., 2005; Soares Júnior et al., 2011).

WHY THERE IS NO SAHARAN ATLANTIC OCEAN

In conclusion, this joint plate kinematic and 3D numerical modelling study elucidates the dynamics of rift competition during the final separation of South America and Africa in the Early Cretaceous. We are able to demonstrate that after ≈20-25 Myrs of coexistence, strain localisation along the EqRS caused the abandonment of the African intraplate rift systems (WARS/CARS) and hence inhibited the formation of a "Saharan Atlantic Ocean" during the Cretaceous. The success of the EqRS was strongly supported by its higher obliquity (60˚) while orthogonal or less oblique extensional domains within the African Plate became inactive. After 20 Myrs of slow rifting, a dramatic increase of the relative extensional velocity between the African and South American plates occurred over a short (≈6 Myrs) period, followed by 6–8 Myrs of fast extension until final separation of the continental lithospheres. Our models suggest that the long period of rift competition and successive weakening was terminated by a severe strength-velocity feedback once the continental bridge between South America and NW Africa had been weakened sufficiently.

Since rift evolution depends heavily on extensional velocity, we propose that the two-stage extension history of the South and Equatorial Atlantic rift system had a large impact on the evolution of the conjugate West African-Brazil margins in the northern and central South Atlantic segments. Our modeled multi-velocity history of the South American plate during continental extension will have exerted a distinct control on the architectural evolution of the conjugate South Atlantic margin segments with an initial slow rifting episode in Pre-Aptian times and subsequent increasing extensional velocities. Our results also call for a re-evaluation of the timing of deformation along the frontier conjugate Equatorial Atlantic margins.

REFERENCES CITED

Artemieva, I. M., 2006, Global 1˚x1˚ thermal model TC1 for the continental lithosphere: Implications for lithosphere secular evolution, *Tectonophysics*, v. *416*, p. 245–277, doi: 10.1016/j.tecto.2005.11.022.

Azevedo, R. P. d. , 1991, Tectonic Evolution Of Brazilian Equatorial Continental Margin Basins [Ph.D. thesis], Department of Geology, Royal School of Mines, Imperial College, Prince Consort Road, London SW7 2BP, 455 p.

Basile, C., J. Mascle, and R. Guiraud, 2005, Phanerozoic geological evolution of the Equatorial Atlantic domain, *J. African Earth Sci.*, v. *43*, p. 275–282, doi:10.1016/j.jafrearsci.2005.07.011.

Bermingham, P. M., J. D. Fairhead, and G. W. Stuart, 1983, Gravity study of the Central African Rift system: a model of continental disruption 2. The Darfur domal uplift and associated Cainozoic volcanism, *Tectonophysics*, v. *94, no.* 1–4, p. 205–222, doi: 10.1016/0040-1951(83)90017-3.

Brownfield, M. E., and R. R. Charpentier, 2006, Geology and Total Petroleum Systems of the Gulf of Guinea Province of West Africa: U.S. Geological Survey Bulletin 2207-C.

Brune, S., and Autin, J., 2013, The rift to break-up evolution of the Gulf of Aden: Insights from 3D numerical lithospheric-scale modelling: Tectonophysics, v. 607, p. 65–79, doi:10.1016/j .tecto.2013.06.029.

Brune, S., A. A. Popov, and S. V. Sobolev, 2012, Modeling suggests that oblique extension facilitates rifting and continental break-up, *J. Geophys. Res.*, v. *117*, no. B8, 402, doi: 10.1029/2011JB008860.

Burke, K., and J. F. Dewey, 1974, Two plates in Africa during the Cretaceous?, *Nature*, v. *249, no.* 5455, p. 313–316.

Chemenda, A., J. Déverchère, and E. Calais, 2002, Three-dimensional laboratory modelling of rifting: application to the Baikal Rift, Russia, *Tectonophysics*, v. *356, no.* 4, p. 253–273, doi: 10.1016/S0040-1951(02)00389-X.

de Matos, R. M. D., 1992, The Northeast Brazilian Rift System, *Tectonics*, v. *11, no.* 4, p. 766–791, doi: 10.1029/91TC03092.

Fairhead, J. D. , 1986, Geophysical controls on sedimentation within the African Rift Systems, *in* L. Frostick, R. Renaut, I. Reid, and J. Tiercelin, eds., *Sedimentation in the African Rifts*: London, Geological Society [London] *Special Publication:* 25, pp. 19–27, doi: 10.1144/GSL.SP.1986.025.01.03.

Fairhead, J. D. , 1988, Mesozoic plate tectonic reconstructions of the central South Atlantic Ocean: The role of the West and Central African rift system, *Tectonophysics*, v. *155, no.* 1-4, p. 181–191, doi: 10.1016/0040-1951(88)90265-X.

Genik, G. J. , 1992, Regional framework, structural and petroleum aspects of rift basins in Niger, Chad and the Central African Republic (C.A.R.), *Tectonophysics*, v. *213, no.* 1-2, p. 169–185, doi: 10.1016/0040-1951(92)90257-7.

Heine, C., J. Zoethout, and R. D. Müller, Kinematics of the South Atlantic rift, *Solid Earth*, v. *4, no.* 2, p. 215–253, doi: 10.5194/se-4-215-2013, 2013.

Janssen, M. E., R. A. Stephenson, and S. Cloetingh, 1995, Temporal and spatial correlations between changes in plate motions and the evolution of rifted basins in Africa. *Geol. Soc. Am. Bulletin v.107*, p. 1317– 1332, doi: 10.1130/0016-7606(1995)107<1317:TASCBC>2.3.CO;2.

Karner, G. D., and N. W. Driscoll, 1999, Tectonic and stratigraphic development of the West African and eastern Brazilian Margins: insights from quantitative basin modelling, *in* Cameron, N. R., Bate, R. H., and Clure, V. S., eds., *The Oil and Gas Habitats of the South Atlantic*: London, Geological Society [London] *Special Publication* 153, p. 11–40, doi:10.1144/GSL.SP.1999.153.01.02.

Labails, C., J.-L. Olivet, D. Aslanian, and W. R. Roest, 2010, An alternative early opening scenario for the Central Atlantic Ocean, *Earth Planet. Sci. Lett.*, v. *297, no.* 3-4, p. 355–368, doi: 10.1016/j.epsl.2010.06.024.

Maloney, K., G. L. Clarke, K. A. Klepeis, and L. Quevedo, (accepted), The Late Jurassic to present evolution of the Andean margin: drivers and the geological record, *Tectonics*, doi: 10.1016/j.epsl.2010.06.024.

Mascle, J., and E. Blarez, 1987, Evidence for transform margin evolution from the Ivory Coast-Ghana continental margin, *Nature*, v. *326, no.* 6111, p. 378–381, doi: 10.1038/326378a0.

McHargue, T. R., T. L. Heidrick, and J. E. Livingston, 1992, Tectonostratigraphic development of the Interior Sudan rifts, Central Africa, *Tectonophysics*, v. *213, no.* 1-2, p. 187–202, doi: 10.1016/0040-1951(92)90258-8.

Moulin, M., D. Aslanian, and P. Unternehr, 2009, A new starting point for the South and Equatorial Atlantic Ocean, *Earth Sci. Rev.*, v. *97*, p. 59–95, doi: 10.1016/j.earscirev.2009.08.001.

Nürnberg, D., and R. D. Müller, 1991, The tectonic evolution of the South Atlantic from Late Jurassic to present, *Tectonophysics*, v. *191, no.* 1-2, p. 27–53, doi: 10.1016/0040-1951(91)90231-G.

Ojo, S. B., 1990, Origin of a major aeromagnetic anomaly in the Middle Niger Basin, Nigeria, *Tectonophysics*, v. *185, no.* 1–2, p. 153–162, doi: 10.1016/0040-1951(90)90410-A.

Petters, S. W., 1981, Stratigraphy of Chad and Iullemmeden basins (West Africa), *Eclogae Geol. Helv.*, v. *74*, no. 1, p. 139–159, doi: 10.5169/seals-165095.

Popov, A. A., and S. V. Sobolev, 2008, SLIM3D: A tool for three-dimensional thermomechanical modeling of lithospheric deformation with elasto-visco-plastic rheology, *Phys. Earth Planet. Int.*, v. *171*, no. 1–4, p. 55–75, doi: 10.1016/j.pepi.2008.03.007.

Ramos, V. A. , 2010, The tectonic regime along the andes: Present-day and mesozoic regimes, *Geological Journal*, v. *45, no.* 1, p. 2–25, doi: 10.1002/gj.1193.

Soares Júnior, A. V., Y. Hasui, J. B. S. Costa, and F. B. Machado, Evolução do Rifteamento e

Paleogeografia da Margem Atlântica Equatorial do Brasil: Triássico ao Holoceno, *Geociências*, v. *30, no.* 4, p. 669–692, 2011.

Torsvik, T. H., R. D. Müller, R. Van der Voo, B. Steinberger, and C. Gaina, 2008, Global Plate Motions Frames: Toward a unified model, *Rev. Geophys.*, v. *46*, p. RG3004, doi: 10.1029/2007RG000227.

Torsvik, T. H., S. Rousse, C. Labails, and M. A. Smethurst, 2009, A new scheme for the opening of the South Atlantic Ocean and the dissection of an Aptian salt basin, *Geophys. J. Int.*, v. *177*, no. 3, p. 1315–1333, doi: 10.1111/j.1365-246X.2009.04137.x.

Unternehr, P., D. Curie, J. L. Olivet, J. Goslin, and P. Beuzart, 1988, South Atlantic fits and intraplate boundaries in Africa and South America, *Tectonophysics*, v. *155, no.* 1-4, p. 169–179, doi: 10.1016/0040-1951(88)90264-8.

Wilson, M., and R. Guiraud, 1992, Magmatism and rifting in Western and Central Africa, from Late Jurassic to Recent times, *Tectonophysics*, v. *213, no.* 1-2, p. 203–225, doi: 10.1016/0040-1951(92)90259-9.

ACKNOWLEDGMENTS

CH is funded by ARC Linkage Project LP0989312 with Shell E&P and TOTAL. SB is funded by SAMPLE, DFG Priority Program 1375 and the ERC, Marie Curie IOF, Project 326115 “GLORY”. We are grateful for the detailed reviews of S. Cloething, M. Moulin and an anonymous reviewer. B. Steinberger and J. Whittaker commented on an earlier version of this manuscript. Figures and plate reconstructions were made using the open source software GMT (http://gmt.soest.hawaii.edu) and GPlates (http://www.gplates.org).

–Methodology background information– Oblique Rifting in the Equatorial Atlantic: Why there is no Saharan Atlantic Ocean

Christian Heine[1]*, Sascha Brune[1,2]†
[1]EarthByte Research Group, School of Geosciences,
The University of Sydney, NSW 2006, Australia
[2]GFZ-Potsdam, Geodynamic Modelling Section, 14473 Potsdam, Germany

1 Numerical model description

1.1 Model setup

We apply the finite element code SLIM3D (Semi-Lagrangian Implicit Model for 3 dimensions; *Popov and Sobolev*, 2008) to solve the coupled system of conservation equations for momentum, thermal energy and constitutive equations that include the effects temperatur- and stress-dependent viscosity and elastic compressibility. Our simulation domain measures 2400 km times 1600 km horizontally and 200 km vertically. We thereby use 192000 cubic elements with a horizontal and vertical dimension of 20 km and 10 km, respectively. The implicit time stepping of the code allows for a step size of 20 ky. The lithospheric segment is vertically divided in four distinct petrological layers: 20 km of felsic upper crust, 20 km of mafic lower crust, 80 km of strong lithospheric mantle, and 80 km of weak asthenospheric mantle. Rheological parameters of the crust (Supplementary Table 1) are chosen to represent a narrow rift setting as it is evident in the Equatorial Atlantic by the short amount of thinned continental crust. The rheology of lithospheric and asthenospheric mantle is based on laboratory creep measurements for dry and wet olivine, respectively.

1.2 Thermal setup

The pattern of Gondwanaland break-up shows that lithospheric extension occurred within mobile belts (*Ziegler and Cloetingh*, 2004). It is still unknown which mechanism is responsible for the mechanical memory of these intracontinental suture zones: inherited faults,

*mailto:christian.heine@sydney.edu.au
†mailto:brune@gfz-potsdam.de

Parameter	Upper Crust	Lower Crust	Strong Mantle	Weak Mantle
Density, ρ ($\mathrm{kg\,m^{-3}}$)	2700	2850	3300	3300
Thermal expansivity, α ($10^{-5}\,\mathrm{K^{-1}}$)	2.7	2.7	3.0	3.0
Bulk modulus, K (GPa)	55	63	122	122
Shear modulus, G (GPa)	36	40	74	74
Heat capacity, C_p ($\mathrm{J\,kg^{-1}\,K^{-1}}$)	1200	1200	1200	1200
Heat conductivity, λ ($\mathrm{W\,K^{-1}\,m^{-1}}$)	2.5	2.5	3.3	3.3
Radiogenic heat production, A ($\mu\mathrm{W\,m^{-3}}$)	1.5	0.2	0	0
Initial friction coefficient, μ (-)	0.6	0.6	0.6	0.6
Maximum plastic friction softening*	90 %	90%	none	none
Cohesion, c (MPa)	5.0	5.0	5.0	5.0
Pre-exponential constant for diffusion creep, $\log(B_{Diff})$ ($\mathrm{Pa^{-1}\,s^{-1}}$)	-	-	-8.65	-8.65
Activation energy for diffusion creep, E_{Diff} ($\mathrm{kJ\,mol^{-1}}$)	-	-	375	335
Activation volume for diffusion creep, V_{Diff} ($10^{-6}\mathrm{m^{-3}/mol}$)	-	-	6	4
Pre-exponential constant for dislocation creep , $\log(B_{Disloc})$ ($\mathrm{Pa^{-n}\,s^{-1}}$)	-28.0	-21.05	-15.56	-15.05
Power law exponent for dislocation creep, n	4.0	4.2	3.5	3.5
Activation energy for dislocation creep, E_{Disloc} ($\mathrm{kJ\,mol^{-1}}$)	223	445	530	480
Activation volume for dislocation creep, V_{Disloc} ($10^{-6}\mathrm{m^{-3}/mol}$)	0	0	13	10

Table 1: Numerical model parameters. Dislocation creep parameters for upper crust: wet quartzite (*Gleason and Tullis*, 1995), lower crust: mafic granulite (*Wilks and Carter*, 1990), strong mantle: dry olivine (*Hirth and Kohlstedt*, 2003), weak mantle: wet olivine, i.e. 500 ppm H/Si (*Hirth and Kohlstedt*, 2003). Olivine grain size is held constant at 6 mm and is included in the pre-exponential factors. *linear decrease of μ from 0.6 to 0.06 between 0 and 1 strain.

crustal lithology, foliations in crustal rocks or anisotropy of olivine crystals in the mantle (*Tommasi and Vauchez*, 2001). However, each of these mechanism leads to local strength reduction and if the suture zone is thrown into extension, all of these processes lead to lithospheric necking and hot asthenospheric upwelling. In our model, we introduce inheritance via a thermal temperature perturbation at the bottom of the mobile belt lithosphere: We position the thermal lithosphere-asthenosphere boundary depth (1350 °C) to 120 km in mobile belts and to 150 km depth in the surrounding plate interiors. Both values are derived from recent compilations of lithosphere thickness in Africa (*Artemieva*, 2006). The initial temperature distribution of the model results from a thermal equilibrium that is defined by material parameters (radiogenic heat production and conductivity, see Supplementary Table 1) and the following boundary conditions: The surface temperature is held constant at 0 °C, whereas below the initial lithosphere-asthenosphere depth, the asthenosphere temperature is set to 1350 °C. Lateral boundaries are thermally isolated. During subsequent model evolution we fix the bottom boundary temperature to 1350 °C allowing for a self-consistent evolution of lithosphere thickness.

1.3 Mechanical boundary conditions

We apply dynamic boundary conditions at the model sides normal to x-direction: During the rift process, the boundary force is kept constant which allows for self-consistent evolution of extensional velocities. This approach is feasible if the model domain comprises a large region whose strength is a major component in the overall force balance of the involved plates. In our case, we assume that the westward motion of the South American plate results from the balance of proto-Andean subduction forces, mantle drag and the resisting strength of the involved rift segments (SARS, EqRS, WARS, CARS). The northern and south-eastern boundaries of the South Atlantic plate consist of low-strength mid ocean ridges. The constant boundary force is maintained in our model until extensional velocities reach typical sea-floor spreading amplitudes. Once this happens, rift strength is so low that it does not contribute to the force balance of the South American plate anymore. Hence, the South American plate velocity results from subduction forces and mantle drag only. This stage is represented in our model by using velocity boundary conditions at the model side facing in x-direction.

For the upper and lower model boundaries we use a free surface and isostatic Winkler support, respectively. During remeshing, the lower boundary is reset to 200 km, whereby Lagrangian markers are either deleted or introduced. Throughout the simulation, boundary conditions in y-direction involve a continuous stress formulation, i.e. the face-parallel components of the stress tensor inside and outside the model domain are forced to be identical while non-zero face-perpendicular velocities are not allowed. This formulation is an extension of the free-slip boundary condition as the latter has the disadvantage that model boundaries are not able to sustain shear stresses and therefore represent enormous vertical faults cutting through the whole lithosphere.

1.4 Weakening mechanisms

Narrow shear zones localize in the model domain generated by three thermo-mechanical weakening feedbacks: (1) Frictional strain softening is implemented via a strain-dependent effective friction coefficient that decreases linearly from 0.6 to 0.06 if the plastic strains increases from 0 and 1 while it remains constant at 0.06 for plastic strains larger than 1. (2) A temperature increase due to viscous and plastic deformation (i.e. shear heating) reduces the viscosity. (3) Nonlinear stress dependence in the dislocation creep law results in strain rate softening and localized viscosity decrease.

However, the strongest weakening effect in our rift models derives from lithospheric thinning and upwelling of hot asthenospheric material (*Brune et al.*, 2012). Since extensional deformation and subsequent necking are attracted to regions of low lithospheric strength, weak lithospheric areas will undergo a pronounced localization feedback.

2 Alternative numerical model setups

In order to test the robustness of our model results, a number of experiments have been conducted where we varied the general rift geometry, the model side where extension is applied, lithosphere and crustal thickness, rheology and initial rift width. All setups lead to the same outcome that the oblique rift is mechanically favored. Here, we depict the simulations where extension is applied to the opposite model side (Supplementary Figure 1-a), where the initial rift configuration is simplified (Supplementary Figure 1-b) and where the competing rift branches do not intersect (Supplementary Figure 1-c).

Applying extension at the opposite model edge (Supplementary Figure 1-a) essentially represents a different motion of the model domain with respect to the asthenosphere. This setup leads to nearly identical model evolution with a slow initial rift phase followed by severe acceleration after 27 My. The similarity between this model and the one shown in Figure 3 (main article) means that asthenospheric flow does not affect our experiments. It also shows that our results are independent of the mantle reference frame that was chosen for the plate tectonic reconstruction.

The complex intersection of the Central African Rift System (CARS) with the West African Rift System (WARS) has been introduced in our numerical setup through a diffuse wide initial rift zone at the North-East Model side. In order to estimate the impact of this wide rift zone on the model dynamics, we conducted an experiment where this zone of complexity was neglected. Only WARS, SARS and EqRS are accounted for with identical initial rift width of 200 km (Supplementary Figure 1-b). The general model evolution is very similar to the model of Figure 3 (main article), but the timing of the individual phases is different. The simplified model experiences strong plate acceleration already after 17 My instead of 27 My like in the original model. The reason for this behavior lies in the dynamics of rift competition. If two competing rifts are similarly strong, like in the reference model where the obliquity of the EqRS is balanced by the wider weak zone of

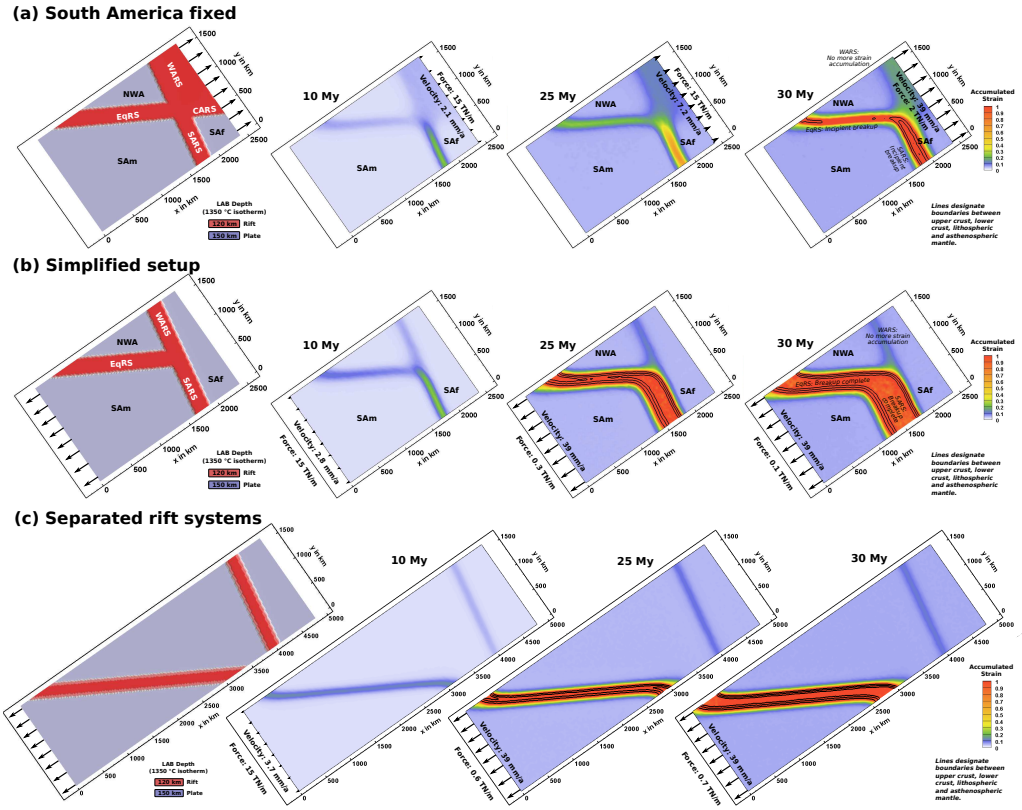

Figure 1: Alternative model scenarios. First image in each line shows the model setup, subsequent images the model's evolution in time in terms of accumulated plastic strain. Rift velocities are depicted by black arrows, the respective value of velocity and force is indicated at the model boundary.

the WARS, each of the rift arms will acquire similar amounts of strain. If the lithosphere of one arm is strengthened significantly (here: WARS), the other rift (EqRS) will accumulate strain at a higher rate leading to more efficient weakening in this rift arm and earlier break-up than in the reference model.

We reduce model complexity by omitting the rift triple-junction. Note that the length of the model has to be enlarged in order to avoid contact of the rift branches. The highly oblique rift arm reaches break-up after 28 My. The model evolution is nearly identical to the previous scenario. These experiments show that our conclusions do not depend on details of the setup.

For even more simplified, fundamental 2D experiments with a single rift zone, we refer to the Section 4.3 of *Brune et al.* (2012). These experiments show the same speed-up for extension rates if force boundary conditions are applied.

References

Artemieva, I. M., Global $1^\circ \times 1^\circ$ thermal model TC1 for the continental lithosphere: Implications for lithosphere secular evolution, *Tectonophysics*, *416*, 245–277, doi: 10.1016/j.tecto.2005.11.022, 2006.

Brune, S., A. A. Popov, and S. V. Sobolev, Modeling suggests that oblique extension facilitates rifting and continental break-up, *Journal of Geophysical Research*, *117*(B8), B08,402, doi:10.1029/2011JB008860, 2012.

Gleason, G. C., and J. Tullis, A Flow Law for Dislocation Creep of Quartz Aggregates Determined with the Molten-Salt Cell, *Tectonophysics*, *247*(1-4), 1–23, 1995.

Hirth, G., and D. L. Kohlstedt, Rheology of the upper mantle and the mantle wedge: A view from the experimentalists, *Geophysical Monograph*, *138*, 83–105, 2003.

Popov, A. A., and S. V. Sobolev, SLIM3D: A tool for three-dimensional thermomechanical modeling of lithospheric deformation with elasto-visco-plastic rheology, *Phys. Earth Planet. Int.*, *171*(1–4), 55–75, doi:10.1016/j.pepi.2008.03.007, 2008.

Tommasi, A., and A. Vauchez, Continental rifting parallel to ancient collisional belts: an effect of the mechanical anisotropy of the lithospheric mantle, *185*, 199–210, doi: 10.1016/S0012-821X(00)00350-2, 2001.

Wilks, K. R., and N. L. Carter, Rheology of Some Continental Lower Crustal Rocks, *Tectonophysics*, *182*(1-2), 57–77, doi:10.1016/0040-1951(90)90342-6, 1990.

Ziegler, P. A., and S. A. P. L. Cloetingh, Dynamic processes controlling evolution of rifted basins, *Earth Sci. Rev.*, *64*(1–2), 1–50, doi:10.1016/S0012-8252(03)00041-2, 2004.